Hydration of the Calcium Ion. An EXAFS, Large-Angle X-ray Scattering, and Molecular Dynamics Simulation Study

Farideh Jalilehvand,[†] Daniel Spångberg,[‡] Patric Lindqvist-Reis,[†] Kersti Hermansson,*[,‡] Ingmar Persson,*[,§] and Magnus Sandström*[,⊥]

Contribution from the Department of Chemistry, Royal Institute of Technology, S-100 44 Stockholm, Sweden, Inorganic Chemistry, The Ångström Laboratory, Uppsala University, P.O. Box 538, S-751 21 Uppsala, Sweden, Department of Chemistry, Swedish University of Agricultural Sciences, P.O. Box 7015, S-750 07 Uppsala, Sweden, and Department of Structural Chemistry, Arrhenius Laboratory, Stockholm University, S-106 91 Stockholm, Sweden

Received May 3, 2000

Abstract: The structure of the hydrated calcium(II) ion in aqueous solution has been studied by means of extended X-ray absorption fine structure spectroscopy (EXAFS), large-angle X-ray scattering (LAXS), and molecular dynamics (MD) methods. The EXAFS data displayed a broad and asymmetric distribution of the Ca−O bond distances with the centroid at 2.46(2) Å. LAXS studies on four aqueous calcium halide solutions (1.5−2 mol dm^{-3}) gave a mean Ca−O bond distance of 2.46(1) Å. This is consistent with a hydration number of 8 determined from correlations between mean distances and coordination numbers from crystal structures. The LAXS studies showed a second coordination sphere with a mean Ca···O_{II} distance of 4.58(5) Å, and for the hydrated halide ions the distances Cl···O 3.25(1) Å, Br···O 3.36(1) Å, and I···O 3.61(1) Å were obtained. Molecular dynamics simulations of $CaCl_2$(aq) were performed using three different Ca^{2+}−OH_2 pair potentials. The potential from the GROMOS program gave results in agreement with experiments, i.e., a coordination number of 8 and an average Ca−O distance of 2.46 Å, and was used for further comparisons. Theoretical EXAFS oscillations were computed for individual MD snapshots and showed very large variations, though the simulated average spectrum from 2000 snapshots gave satisfactory agreement with the experimental EXAFS spectra. The effect of thermal motions of the coordinated atoms is inherent in the MD simulation method. Thermal disorder parameters evaluated from simulated spatial atom distribution functions of the oxygen atoms coordinated to the calcium ion were in close agreement with those from the current LAXS and EXAFS analyses. The combined results are consistent with a root-mean-square displacement from the mean Ca−O distance of 0.09(2) Å in aqueous solution at 300 K.

1. Introduction

The hydrated calcium ion, which is present in a concentration close to 1 mmol·dm^{-3} in extracellular fluids, has a diversity of important roles in the biochemical functions of the human body, e.g., in control of metabolism, muscle contraction, blood clotting, cell division, and hormonal activities.[1] The binding properties, the flexibility, and fast kinetics of its coordination make the calcium ion suitable for controlling conformational changes in the biochemical processes of the cell. The coordination geometry is often irregular and is strongly influenced by the second coordination sphere.[1] The great biochemical importance of the calcium ion has led to a number of structural studies to determine its hydration in aqueous solution. However, this is a notoriously difficult problem because of the flexibility of the first coordination sphere and the low atomic number of the atoms involved. Interpretation of the experimental data from various techniques has given results with large variations.[2]

High concentrations of calcium are necessary for diffraction studies in aqueous solution. The Ca−O bond distances obtained by means of the large-angle X-ray scattering (LAXS) method are around 2.4 Å, and a hydration number of 6 is proposed.[2] A coordination number of 6.9(5) has also been reported, with the Ca−O bond distance 2.39(1) Å.[3] From a neutron diffraction study on concentrated aqueous solutions of calcium chloride, it was concluded that the coordination number and configuration are concentration-dependent,[4] but this has not been confirmed by other studies. LAXS data from calcium chloride hydrate melts, $CaCl_2$·nH_2O, $4.0 < n < 8.6$, showed the mean Ca−O distance 2.45 Å, which was interpreted as indicating six coordination and that calcium−chloride contact ion pairs were formed with Ca−Cl distances of 2.7 Å when $n \leq 6$.[5] For very concentrated calcium nitrate solutions, $Ca(NO_3)_2$·mH_2O with $m = 6$ and 12, seven coordination with the Ca−O distance 2.47 Å, including the formation of inner-sphere ion pairs between the calcium ion and one nitrate ion, was proposed.[6]

* Corresponding authors.
† Royal Institute of Technology.
‡ Uppsala University.
§ Swedish University of Agricultural Sciences.
⊥ Stockholm University.

(1) Frausto da Silva, J. J. R.; Williams, R. P. J. *The Biological Chemistry of the Elements*; Clarendon: Oxford, 1991; Chapter 10.
(2) Ohtaki, H.; Radnai, T. *Chem. Rev.* **1993**, *93*, 1157 and references therein.
(3) Probst, M. M.; Radnai, T.; Heinzinger, K.; Bopp, P.; Rode, B. M. *J. Phys. Chem.* **1985**, *89*, 753.
(4) Hewish, N. A.; Neilson, G. W.; Enderby, J. E. *Nature* **1982**, *297*, 138.
(5) Yamaguchi, T.; Hayashi, S.; Ohtaki, H. *Inorg. Chem.* **1989**, *28*, 2434.
(6) Smirnov, P.; Yamagami, M.; Wakita, H.; Yamaguchi, T. *J. Mol. Liq.* **1997**, *73*−*74*, 305.
(7) Kollman, P. A.; Kuntz, I. D. *J. Am. Chem. Soc.* **1972**, *94*, 9236.

10.1021/ja001533a CCC: $20.00
Published on Web 12/23/2000

Theoretical studies of the calcium ion−water interaction have been performed using ab initio methods,[7−12] Monte Carlo (MC) simulations,[13] and molecular dynamics (MD) simulations.[3,14−21] Density functional theory (DFT) and free energy MC calculations have been used to compare the stability of different Ca^{2+}−water clusters. DFT calculations with large basis sets showed marginally higher stability for the isolated $Ca(OH_2)_6^{2+}$ species (mean Ca−O bond distance 2.37 Å) than for $Ca(OH_2)_7^{2+}$ (mean Ca−O 2.41 Å) and $Ca(OH_2)_8^{2+}$ (mean Ca−O 2.48 Å in a wide distribution).[12] However, the DFT calculations correspond to gas-phase conditions at 0 K. At ambient temperature the additional space requirement, due to the increasing thermal and configurational disorder of the water molecules, is likely to destabilize the lower hydration numbers with the closest ligand−ligand contacts. This is consistent with the coordination numbers obtained by means of MC and MD methods, which vary between 7.0 and 9.3 for Ca^{2+}−O distances in the range 2.39−2.54 Å. A recently published MD study of the hydrated calcium ion in solution, where thermodynamic and dynamic properties were calculated by using different Ca^{2+}−water potentials, concluded that the lack of accurate experimental information makes it difficult to select the most reliable potential.[21]

In the present study, both the extended X-ray absorption fine structure spectroscopy (EXAFS) and the large-angle X-ray scattering (LAXS) methods have been used to obtain information about the local structure around the hydrated calcium(II) ion. The EXAFS functions normally cover a larger range of the scattering variable than in LAXS because of the backscattering of the ejected photoelectron.[22,23] This increases the resolution and allows evaluation of possible configurational disorder or asymmetric distributions of the metal−oxygen distances in the first coordination sphere. In the current EXAFS study, theoretically calculated model functions, including the third phase-shifting cumulant in an expansion describing an asymmetric distribution of the Ca−O distances,[23] were fitted to the experimental EXAFS spectra. However, the high X-ray absorption by the solvent at the Ca K-edge made it necessary to use concentrated solutions and to collect EXAFS data in the fluorescence mode.

High concentration is also necessary for the LAXS studies, since the scattering of other atom pairs not involving the metal ion partly overlaps with the relatively weak scattering contribution from the calcium−oxygen distances. Therefore, solutions with different concentrations and with anions of different sizes, i.e., chloride, bromide, and iodide, were used in the present study in order to get a consistent description of the calcium hydration. Calcium perchlorate solutions could be used for the EXAFS but not for the LAXS studies since the O···O distances within the perchlorate ion severely overlap the Ca—O bond distance. To evaluate the LAXS data, the structure of the hydrated halide ions in aqueous solution also had to be described. Ohtaki and Radnai have reviewed previous results from large-angle X-ray or neutron scattering.[2] The Cl···O, Br···O, and I···O distances were found to be in the ranges 3.1−3.25, 3.3−3.4, and 3.6−3.7 Å, respectively, with a wide distribution in the results from different systems. For the theoretical modeling of the LAXS data, it is only possible to consider symmetric distributions of the interatomic distances described by a Debye−Waller factor, $\exp(-2\sigma_1^2 s^2)$, cf. eq 3.[22,23] On the other hand, the LAXS data for low s values allow the long-range second-sphere interactions to be studied, which is not possible using EXAFS on this type of disordered system.[24] Both techniques can give fairly precise mean metal−oxygen bond distances but not very accurate coordination numbers.

In parallel, MD simulations of aqueous calcium chloride solutions with different concentrations have been performed to obtain structural details that are not easily available from the experimental methods. Different calcium ion−water pair potentials were tested. Theoretical EXAFS spectra were also computed. For this purpose, the atomic positions of 2000 different configurations from the MD simulations were used to generate a separate Ca K-edge EXAFS oscillation for each individual atomic configuration by means of the same computer program (FEFF)[25] as was used for the analysis of the experimental EXAFS spectra. By adding up the individual computed oscillations, simulated EXAFS spectra were obtained and compared with the experimental spectra.

The average coordination figures of the calcium ion−water complexes formed in the MD data sets were evaluated by using spatial distribution functions.[26] The "thermal disorder parameters", expressing the average displacement of the water molecules from their equilibrium bond distance, were computed from the spatial distribution functions and compared with the experimental disorder parameters.

2. Experimental and Computational Details

2.1. Sample Preparation. The EXAFS spectra were measured on calcium chloride (slightly acidified) and perchlorate solutions, and the LAXS measurements were performed on aqueous calcium chloride, bromide, and iodide solutions (Table 1). The calcium bromide, iodide, and perchlorate solutions were prepared by dissolving calcium oxide (Merck) in hydrobromic, hydroiodic, or perchloric acid (Merck), giving acidic solutions. The calcium chloride and the dilute bromide solutions were obtained by dissolving calcium chloride dihydrate (Merck) and anhydrous calcium bromide (Aldrich), respectively, in deionized water. The calcium content of all solutions was determined by EDTA titration

(8) Ortega-Blake, I.; Barthelat, J. C.; Costes-Puech, E.; Oliveros, E.; Daudey, J. P. *J. Chem. Phys.* **1982**, *76*, 4130.
(9) Ortega-Blake, I.; Novaro, O.; Lés, A.; Rybak, S. *J. Chem. Phys.* **1982**, *76*, 5405.
(10) Waizumi, K.; Masuda, H.; Fukushima, N. *Inorg. Chim. Acta* **1993**, *209*, 207.
(11) Katz Kaufmann, A.; Glusker, J. P.; Beebe, S. A.; Bock, C. W. *J. Am. Chem. Soc.* **1996**, *118*, 5752.
(12) Pavlov, M.; Siegbahn, P. E. M.; Sandström, M. *J. Phys. Chem. A* **1998**, *102*, 219.
(13) Bernal-Uruchurtu, M. I.; Ortega-Blake, I. *J. Chem. Phys.* **1995**, *103*, 1588.
(14) Bounds, D. G. *Mol. Phys.* **1985**, *54*, 1335.
(15) Åquist, J. *J. Phys. Chem.* **1990**, *94*, 8021.
(16) Floris, F. M.; Persico, M.; Tani, A.; Tomasi, J. *Chem. Phys. Lett.* **1994**, *227*, 126.
(17) Floris, F. M.; Persico, M.; Tani, A.; Tomasi, J. *Chem. Phys.* **1995**, *195*, 207.
(18) Obst, S.; Bradaczek, H. *J. Phys. Chem.* **1996**, *100*, 15677.
(19) Tongraar, A.; Liedl, K. R.; Rode, B. M. *J. Phys. Chem. A* **1997**, *101*, 6299.
(20) Koneshan, S.; Rasaiah, J. C.; Lynden-Bell, R. M.; Lee, S. H. *J. Phys. Chem. B* **1998**, *102*, 4193.
(21) Guardia, E.; Sese, G.; Padro, J. A.; Kalko, S. G. *J. Solution Chem.* **1999**, *28*, 1113.
(22) Persson, I.; Sandström, M.; Yokoyama, H.; Chaudhry, M. *Z. Naturforsch.* **1995**, *50a*, 21.
(23) Crozier, E. D.; Rehr, J. J.; Ingalls, R. In *X-Ray Absorption, Principles, Applications, Techniques of EXAFS, SEXAFS, and XANES*; Koningsberger, D. C., Prins, R., Eds.; Wiley-Interscience: New York, 1988; Chapter 9.
(24) Lindqvist-Reis, P.; Muñoz-Páez, A.; Díaz-Moreno, S.; Pattanaik, S.; Persson, I.; Sandström, M. *Inorg. Chem.* **1998**, *37*, 6675.
(25) (a) FEFF code for ab initio calculations of XAFS: Zabinsky, S. I.; Rehr, J. J.; Ankudinov, A.; Albers, R. C.; Eller, M. J. *Phys. Rev. B* **1995**, *52*, 2995. Ankudinov, A. Ph.D. Thesis, University of Washington, 1996. (Version 6 used for the MD simulations, version 7 for the EXAFS data.) (b) Rehr, J. J.; Ankudinov, A.; Zabinsky, S. I. *Catal. Today* **1998**, *39*, 263.
(26) Laaksonen, A.; Kusalik, P. G.; Svishhev, I. M. *J. Phys. Chem.* **1997**, *101*, 5910.
(27) Schwarzenbach, G.; Flaschka, H. *Die Komplexometrische Titration*; Ferdinand Enke: Stuttgart, 1965.

Table 1. Composition (mol·dm^{-3}) of the Aqueous Calcium Solutions Studied by LAXS and EXAFS[a]

sample	label	[Ca^{2+}]	[X^-]	[H^+]	[H_2O]	ρ (g·cm^{-3})	μ (cm^{-1})	method
CaI_2	I1	1.50	3.10	0.10	48.2	1.318	16.6	LAXS
$CaBr_2$	BR1	1.49	2.98	*b*	51.7	1.229	21.2	LAXS
$CaBr_2$	BR2	2.00	4.40	0.40	46.8	1.275	30.5	LAXS
$CaCl_2$	CL2	2.01	4.02	*b*	50.7	1.137	4.2	LAXS
$CaCl_2$		1.50	3.00	*b*				EXAFS
$Ca(ClO_4)_2$		1.88	3.77	(pH = 2)				EXAFS
$Ca(ClO_4)_2$		0.94	1.89	(pH = 2.3)				EXAFS

[a] The density ρ and the linear absorption coefficient μ are given for Mo Kα radiation. [b] No acid added.

using Eriochrome black T as indicator,[27] and the densities were measured with an Anton Paar DMA 35 densitometer. The composition of the solutions is given in Table 1.

2.2. EXAFS Data. The Ca K-edge EXAFS data were measured in fluorescence mode using a Lytle detector without filter at the wiggler beam line 4-1 of the Stanford Synchrotron Radiation Laboratory (SSRL) on two separate occasions. SSRL operates at 3.0 GeV and a maximum current of 100 mA. The EXAFS station was equipped with an Si[111] double-crystal monochromator, and higher order harmonics were discarded by detuning the second monochromator crystal to 30% of maximum intensity at the end of the scans. The experiment was set up in a helium atmosphere in order to minimize air absorption and scattering. The solutions were kept in Teflon cells with windows of thin (6 μm) polypropylene film. For each sample, three or four scans were recorded. They were calibrated and averaged by means of the EXAFSPAK program package.[28]

For energy calibration of the spectra, normally a foil of the metal is used. However, because of the reactivity of calcium metal, the Ca K-edge EXAFS spectra of the solid compounds CaO and $Ca(OH)_2$ with known structures were measured and analyzed instead, with a different compound at each occasion. The same shift of the threshold energy, ΔE_0, was used for the solutions as that obtained from the analysis of the solid with known Ca−O distance, measured on the same occasion.

The EXAFS spectra (Figure 1) were obtained after performing standard procedures for preedge subtraction, normalization, and spline removal by means of the WinXAS software.[29] A model function for the first shell, $\chi_{CaO}(k)$, was made by using ab initio calculated phase $\phi_{Ca,O}(k)$, amplitude $f_{eff}(k)$, and mean-free-path $\lambda(k)$ parameters computed by the FEFF7 program[25] and was curve-fitted to the k^3-weighted data (k is the scattering variable):

$$\chi_{CaO}(k) = \frac{n_O {S_0}^2}{k {d_{CaO}}^2} |f_{eff}(k)|_O \exp(-2k^2 {\sigma_e}^2) \exp[-2d_{CaO}/\lambda(k)] \times \sin[2kd_{CaO} + \phi_{Ca,O}(k) - ({}^4/_3)C_3k^3] \quad (1)$$

The number of oxygen atoms is denoted n_O, the mean (or centroid for an asymmetric distribution)[30] distance in a shell d_{CaO}, and its root-mean-square (rms) displacement σ_e in a Debye−Waller factor. The amplitude reduction factor ${S_0}^2$ has an unknown value, normally between 0.8 and 1.0.[25b] The asymmetry of the Ca−O shell was modeled using a cumulant expansion of the distribution, including the third cumulant, C_3, which compensates for phase shifts in the EXAFS function (Table 2), and also the amplitude-adjusting forth cumulant (Table S2).[23,30] A Bessel window was used for the Fourier transformation with the k-range given in Table 2.

2.3. LAXS Data. The large-angle X-ray scattering measurements were made from the free surface of the solutions, using Bragg−Brentano symmetrical $\theta-\theta$ geometry.[31] Intensity data were collected at 450 discrete θ values in the range $1 < \theta < 65°$ using Mo Kα radiation (λ = 0.7107 Å), which corresponds to a range of 0.3−16.0 Å^{-1} of the scattering variable $s = 4\pi\lambda^{-1} \sin\theta$. At least 100 000 counts were accumulated at every preset angle in two separate scans. The details of the data collection and correction procedures can be found elsewhere.[24,32] The KURVLR program was used for the data treatment.[33] By Fourier transformation of the structure-dependent part of the intensity function, $i(s)$, normalized to a unit of volume chosen to contain one calcium ion, a modified electronic radial distribution function, $D(r)$, is obtained (Figure 2):

$$D(r) = 4\pi r^2 \rho_o + 2r/\pi \int_{S_{min}}^{S_{max}} si(s)\, M(s) \sin(sr)\, ds \quad (2)$$

The modification function $M(s) = [f_{Ca}(s=0)^2/f_{Ca}(s)^2] \exp(-0.008s^2)$ increases the resolution and reduces termination effects, ρ_o is the average electronic scattering density, and f is the atomic X-ray scattering factor.[33] The $i(s)$ function was corrected for oscillations with long periods corresponding to spurious peaks below 1 Å in the $D(r)$ function, which were removed by means of a Fourier back-transformation procedure[34] and analyzed by means of a model function, $i_{calc}(s)$, containing the intensity contributions from atomic pair interactions pq within structural units in the solution:

$$i_{calc}(s) = \sum_p \sum_q (f_p' f_q' + \Delta f_p'' \Delta f_q'') \exp(-2{\sigma_l}^2 s^2) \sin(sr_{pq})/(sr_{pq}) \quad (3)$$

The parameters characterizing the interatomic interactions are r_{pq}, the average distance of separation between the atoms p and q; ${\sigma_l}^2$, the mean-square deviation from the mean distance; and n_{pq}, the number of interactions (see Table 3). Anomalous dispersion corrections, $\Delta f'$ and $\Delta f_p''$, are included in the atomic scattering factor expression ($f' = f_0 + \Delta f'$). All summations are made over a unit of volume containing one calcium atom.

Least-squares refinements of the structural parameters were performed by means of the STEPLR program for well-defined short-range atom pair interactions with water molecules: the Ca−O_I bonds and the $X^-\cdots O_w$ and $O_w\cdots O_w$ hydrogen-bonded interactions.[35] The $si_{calc}(s)$ model function was fitted to the experimental $si(s)$ function for s values larger than 4−5 Å^{-1}; in this range, the contributions from long and/or diffuse (high mean-square deviation ${\sigma_l}^2$) interactions in the solution can be neglected.[22] Model fitting of the second-sphere interactions around the calcium ion was made in r space by fitting Fourier-transformed peak shapes, and by adjusting the structural parameters of the corresponding intensity contributions (eq 2) within reasonable limits.

2.4. MD Data. 2.4.1. Interatomic Potentials. The water−water potential used for the simulations was Jorgensen's TIP4P potential for pure bulk water.[36] TIP4P places a charge of +0.52e at each hydrogen nucleus, a charge of −1.04e 0.15 Å away from the oxygen toward the hydrogen atoms, and a Lennard-Jones site at the oxygen nucleus. The O−H distance is 0.9572 Å, and the H−O−H angle is 104.52°. Three different $Ca^{2+}-OH_2$ interaction potentials were used, namely those of Åquist[15] and Bounds[14] and that supplied with the GROMOS program.[37] The $Cl^- - H_2O$ potential was taken from Bounds,[14] the $Ca^{2+}-Cl^-$ potential from Probst et al.,[3] and the $Cl^- - Cl^-$ potential from Sangster

(28) George, G. N.; Pickering, I. J. *EXAFSPAK—A Suite of Computer Programs for Analysis of X-ray Absorption Spectra*; SSRL: Stanford, CA, 1993.
(29) Ressler, T. *J. Synchrotron Radiat.* **1998**, *5*, 118.
(30) Bunker, G. *Nucl. Instrum. Methods* **1983**, *207*, 437.
(31) Klug, H. P.; Alexander, L. E. *X-ray Diffraction Procedures for Polycrystalline and Amorphous Materials*; Wiley: New York, 1974; Chapter 5.
(32) Ståhlandske, C. M. V.; Persson, I.; Sandström, M.; Kamienska-Piotrowicz, E. *Inorg. Chem.* **1997**, *36*, 3174 and references therein.
(33) Johansson, G.; Sandström, M. *Chem. Scr.* **1973**, *4*, 195.
(34) Levy, H. A.; Danford, M. D.; Narten, A. H. *Data Collection and Evaluation with an X-Ray Diffractometer Designed for the Study of Liquid Structure*; Technical Report ORNL-3960; Oak Ridge National Laboratory: Oak Ridge, TN, 1966.
(35) Molund, M.; Persson, I. *Chem. Scr.* **1985**, *25*, 197.

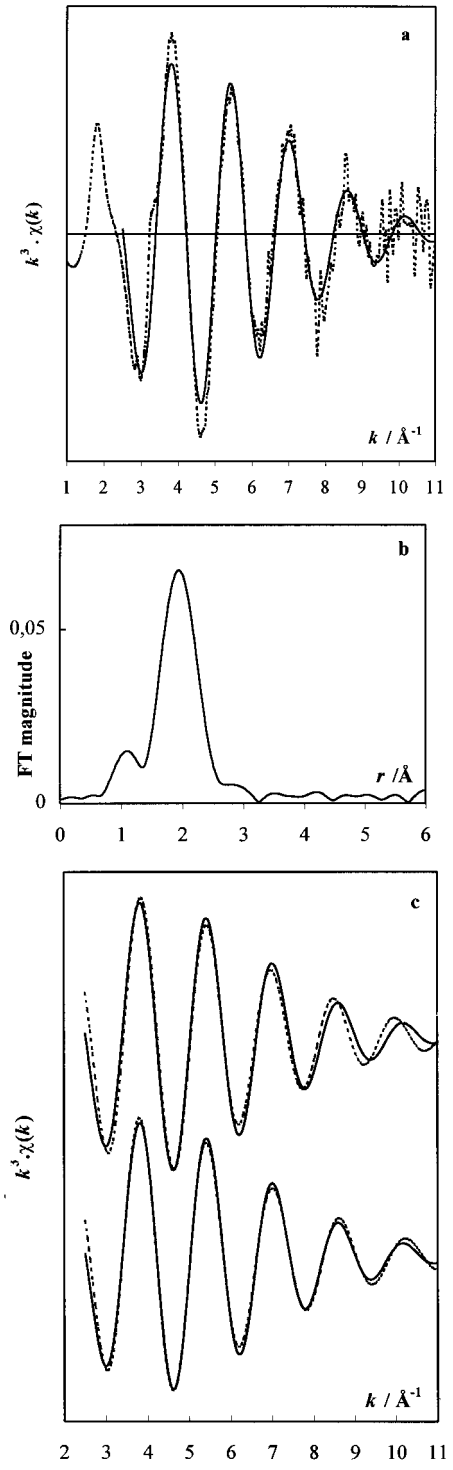

Figure 1. (a) Experimental Ca K-edge EXAFS data for 0.94 mol dm^{-3} $Ca(ClO_4)_2$ aqueous solution (dashes), and back-transform (solid line) of the Ca−O peak in b (r range 1.34−2.68 Å). (b) Fourier transform (k range 2.5−11.0 Å^{-1}, Bessel window, no phase correction). Note that the r scale is shifted about 0.5 Å due to the phase shift. (c) Model (dashes) fitting to the back-transform of the Ca−O peak, assuming symmetric (top curve) and asymmetric distribution (bottom) with parameters from Table 2.

and Atwood.[38] No non-Coulombic $Ca^{2+}-Ca^{2+}$ potential was used since it was expected that the distance between the calcium ions would never be short. The simulation of the most concentrated solution confirmed this, and the shortest $Ca^{2+}\cdots Ca^{2+}$ distance ever occurring was 5.9 Å.

2.4.2. MD Simulations. Simulations with the different $Ca^{2+}-OH_2$ interaction potentials and at different concentrations were performed in the NPT ensemble,[39−41] at zero external pressure and 300 K. Ewald summations were used for the Coulombic interactions.[42] Short-range forces were cutoff at 12 Å. The time step used was 0.75 fs. A predictor−corrector integration algorithm was used to obtain the trajectories.[43] Each system was equilibrated for 7.5 ps, and the production runs were all 15 ps. A cubic simulation box containing 512 particles was used in all cases; see Table 4 for details.

Radial pair distribution functions, g(r), were computed from the MD trajectories, according to eq 4, where $n_O(r)$ is the number of oxygen

$$g_{Ca^{2+}-O}(r) = n_O(r)/(\rho_{ox}\, dV(r)) \qquad (4)$$

atoms in a small spherical shell at a distance r from the Ca^{2+} ion, $dV(r)$ is the volume of this shell, and ρ_{ox} is the number density of oxygen atoms in the solution.

2.4.3. Spatial Distribution Functions. Spatial distribution functions were computed in several steps. In the first step, a cube with side a, typically 6 Å, was created. This cube was divided into n^3 cells (n cells per side). A variable n_{cell} was assigned to each cell to count the number of oxygen atoms located in that particular cell during the course of the simulation. Thus, for every mth time step, all oxygen atoms which were closer than $a/2$ to the ion were selected. The cation and its coordination figure were then translated to place the ion in the middle of the cube, at coordinate ($a/2$, $a/2$, $a/2$). The cell number corresponding to each oxygen atom was determined, and the corresponding cell counters increased by one. For all MD snapshots (except the first one), an additional step was performed before the counting update took place. The coordination figure was rigid-body-rotated to maximize "the overlap" between the current configuration and the previous one, i.e., to attempt to eliminate the effects of rigid-body rotation of the coordination figure. For this purpose, eq 5 was maximized, where n_i is

$$\text{overlap} = \sum_{i=1}^{n_{cell}} \frac{n_i}{|\vec{r}(\text{cell } i) - \vec{r}(\text{closest O}) + C|^2} \qquad (5)$$

the number of accumulated hits for cell i and $|\vec{r}(\text{cell } i) - \vec{r}(\text{closest O})|$ is the distance between the center of cell i and the closest oxygen atom to the cell. C is a constant to avoid division by zero, chosen to be equal to 1. The resulting spatial distributions from each MD run were then analyzed by locating each group of cells, after removing all cells containing fewer hits than some threshold value (50% "probability"). The grouping was made by using a three-dimensional recursive fill algorithm. The position of the maximum value and the total occupancy of each group were computed. Spatial distribution functions were generated by placing a number of spheres in space for each cell and drawing these spheres with the Y_{mol} program.[44] The number of spheres is proportional to the density in the cell.

Thermal ellipsoids were calculated by fixing the ellipsoid centers at the position of the maximum value of each group of cells. For each group, an ellipsoid was then constructed so that all cells belonging to that group were inside the ellipsoid, at the same time keeping the ellipsoid as small as possible. Each ellipsoid was described by the lengths of its principal axes, r_1, r_2, r_3 (with $r_1 < r_2 < r_3$), and a rotation matrix, **R**, with respect to a space-fixed coordinate system. The smallest possible ellipsoid that still contains all points in the group was obtained

(36) Jorgensen, W. L.; Chandrasekar, J.; Madura, J. D.; Impey, R. W.; Klein, M. L. *J. Chem. Phys.* **1983**, *79*, 926.

(37) van Gunsteren, W. F.; Berendsen, H. J. C. *GROningen MOlecular Simulation (GROMOS) package*; available from Biomos n.v. Ninborgh 16, 4767 AG Groningen, The Netherlands, 1987. The Lennard-Jones pair potential used for the Ca−water interaction between Ca and O is $U_{LJ} = 4\epsilon((\sigma/r)^{12} - (\sigma/r)^6)$, where $\sigma = 2.9843$ Å and $\epsilon = 0.573663$ kJ mol^{-1}.

(38) Sangster, M. J. L.; Atwood, R. M. *J. Phys. C: Solid State Phys.* **1978**, *11*, 1541.

(39) Andersen, H. C. *J. Chem. Phys.* **1980**, *72*, 2384.

(40) Nosé, S. *Mol. Phys.* **1984**, *52*, 255.

(41) Hoover, W. G. *Phys. Rev.* **1985**, *A31*, 1695.

(42) Ewald, P. *Ann. Phys.* **1921**, *64*, 253.

(43) Gear, C. W. *Numerical initial value problems in ordinary differential equations*; Prentice-Hall: Englewood Cliffs, NJ, 1971.

(44) Spångberg, D. *Ymol: A molecular visualisation and animation program for the X Window system*; 1998.

Table 2. EXAFS *k* Space Model Fitting (Eq 1, Fourier-Filtered k^3-Weighted Data) of Ca−O Bond Distances[a]

sample	*k* range (Å^{-1})	*n*[b]	*d* (Å)[c]	σ_e^2 (Å^2)	C_3 (Å^3)	ΔE_o (eV)	S_o^2	residual[d]
CaO(s)	2.7−9.9	6	2.398	0.008(1)		6.0(1)	0.42(2)	20.5
$CaCl_2$ (1.5 mol dm^{-3})	3.4−9.6	8	2.435(6)	0.012(2)		6.0[b]	0.82(7)	14.2
	3.4−9.6	8	2.461(9)	0.011(1)	0.0011(3)	6.0[b]	0.81(7)	5.5
$Ca(OH)_2$(s)	3.4−11.4	6	2.374(8)	0.007(1)		5.0(8)	0.40(4)	17.8
$Ca(ClO_4)_2$ (1.88 mol dm^{-3})	2.5−10.0	8	2.426(4)	0.012(1)		5.0[b]	0.83(6)	20
	2.5−10.0	8	2.457(7)	0.011(1)	0.0013(3)	5.0[b]	0.83(5)	7.1
$Ca(ClO_4)_2$ (0.94 mol dm^{-3})	2.5−11.0	8	2.425(4)	0.012(1)		5.0[b]	0.89(6)	20.4
	2.5−11.0	8	2.453(8)	0.012(1)	0.0012(3)	5.0[b]	0.90(6)	9.3

[a] The parameters are coordination number *n*, bond distance *d*, mean square deviation of Ca−O distance σ_e^2, third (phase adjustment) cumulant C_3 for asymmetric distance distribution, threshold shift ΔE_o, and amplitude reduction factor S_o^2. [b] Fixed parameter. [c] Standard deviations (within brackets) for refined parameters are estimated from noise level at high *k* of the zero-weighted $\chi(k)$ (cf. eq 1) and do not include systematic errors (see section 3.1.1). [d] Residual $= \sum_{i=1}^{N}[\chi_{exp}(i) - \chi_{model}(i)]/\sum_{i=1}^{N}\chi_{exp}(i)$.

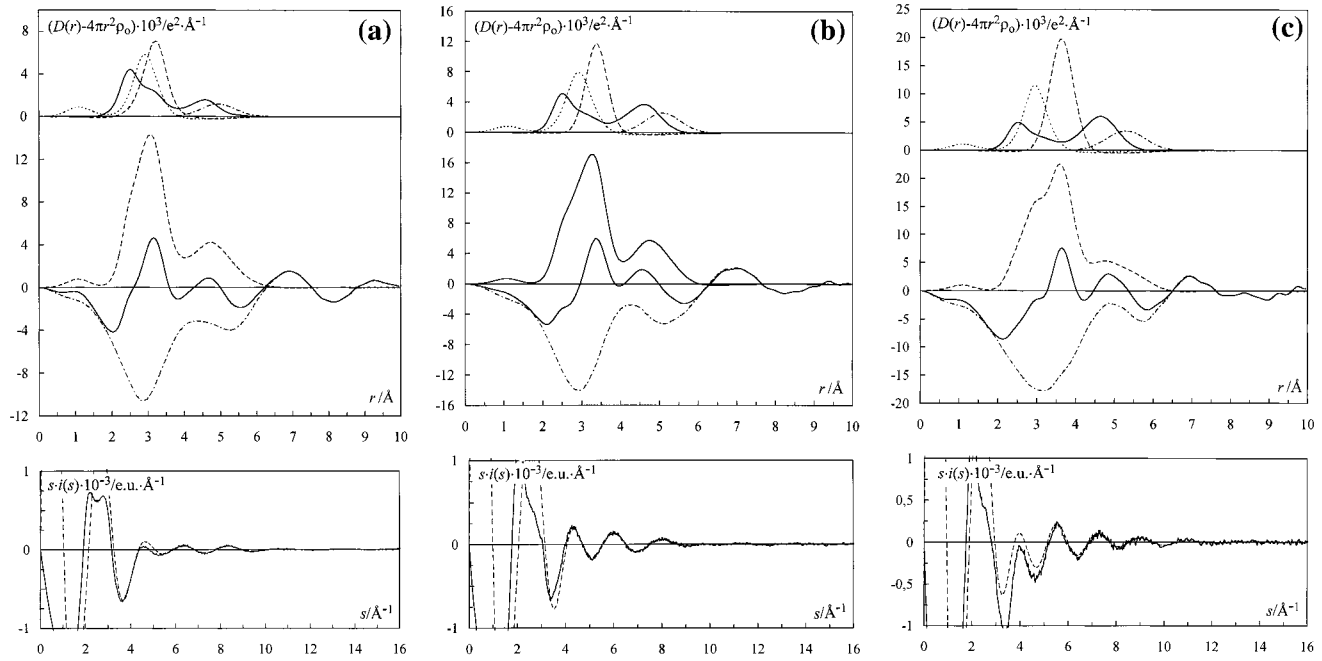

Figure 2. (a) (Top) LAXS radial electronic distributions (RDF) for a 2.0 mol·dm^{-3} $CaCl_2$ solution (CL2). (Upper part) Separate model peak shapes (Table 3): the eight-hydrated calcium ion with the first and second sphere (solid line), the hydrated chloride ion (dashed line) and $O_I\cdots O_{II}$ interactions (dotted line). The dash−dotted line shows the contributions from two chloride ions in the second shell. (Middle) Experimental RDF: $D(r)-4\pi r^2\rho_o$ (solid line); sum of model contributions (dashed line); difference (dash−dotted line). (Bottom) LAXS structure-dependent intensity functions $si(s)$ (solid line); model $si_{calc}(s)$ (dashed line). (b) RDF's for a 2.0 mol·dm^{-3} $CaBr_2$ solution (BR2) with same notation. (c) RDF's for a 1.5 mol·dm^{-3} CaI_2 solution (I1) with same notation.

by minimizing its volume by varying the lengths of the axes and the rotation matrix; the latter was achieved by varying two angles over all space.

Mean-square displacement parameters, $\langle u_j^2\rangle$, for the first-shell oxygen atoms were computed using the formula $\langle u_j^2\rangle = (\langle r_j\rangle/1.5382)^2$, where $\langle r_j\rangle$ for the principal axis *j* ($j = 1, 2, 3$) is the average of r_j taken over the oxygen ellipsoids resulting from the simulation run. The factor 1.5382 corresponds to the surface of 50% constant probability.[45] In this way, "typical" mean-square displacements, $\langle u_j^2\rangle$, and rms displacements, $\langle u_j^2\rangle^{1/2}$ ($=\sigma$) for the first-shell water oxygen atoms were obtained in the MD-simulated aqueous solution. It should be emphasized that it is the oxygen motion relative to the calcium position that is displayed, i.e., the variation of the Ca−O distance, which is the same quantity as that obtained from the fitting of the EXAFS and LAXS data. This differs from thermal parameters obtained from single-crystal diffraction determinations, where individual atomic parameters are usually refined without considering the correlation between the motions of different atoms.[46]

The ellipsoids were visualized by using ORTEP-III.[47] For this purpose, the matrix of anisotropic temperature factors, **A**, was obtained using the relationship $\mathbf{A} = \mathbf{RDR}^T$, where **R** is the rotation matrix (see above) and **D** is the diagonal matrix, diag(r_1^2,r_2^2,r_3^2).

2.4.4. MD Simulation of EXAFS Spectra. EXAFS oscillations were calculated by using the FEFF6 program,[25] taking the calcium ion and the oxygen atom positions from the MD snapshots which were obtained using Bounds's or the GROMOS potentials. Figure 3a−c shows three EXAFS oscillations for a set of configurations computed with the GROMOS potential, taken from the same simulation, 7.5 fs apart. Temperature averaging was performed by averaging EXAFS oscillations computed from a number of consecutive snapshots. The result from averaging 2000 such "instantaneous" EXAFS spectral contributions (as in Figure 3a−c) is shown in Figure 3d.

In the MD-generated spectra displayed in this paper, the Fermi energy level was corrected with −1.8 eV, except for Bounds's potential, where a correction of −2.5 eV was used. Scale factors, 0.58 and 0.53 for the potentials from GROMOS and Bounds, respectively, were used for the adjustment of the theoretical amplitude.

(45) Willis, B. T. M.; Pryor, A. W. *Thermal Vibrations in Crystallography*; University Printing House: Cambridge, Great Britain, 1975.

(46) Trueblood, K. N. In *Accurate Molecular Structures, Their Determination and Importance*; Domenciano, A., Hargittai, I., Eds.; IUCr Monographs on Crystallography 1; Oxford University Press: New York, 1992; Chapter 8.

(47) Burnett M. N.; Johnson C. K. *ORTEP-III: Oak Ridge Thermal Ellipsoid Plot Program for Crystal Structure Illustrations*; Oak Ridge National Laboratory Report ORNL-6895; Oak Ridge National Laboratory, Oak Ridge, TN, 1996.

Table 3. LAXS Model Fitting (Eq 3) for the Calcium Halide Solutions[a]

sample	label	distance	n^b	d (Å)	σ_l^2 (Å^2)
CaI_2(aq)	I1	Ca—O	8	2.46(1)	0.007(1)
		Ca···O_{II}	13(2)	4.58(5)	0.04(1)
		Ca···I	2	5.25(10)	0.05(2)
		I···O	8	3.61(1)	0.016(2)
		O_w···O_w	2	2.93(2)	0.008(2)
$CaBr_2$(aq)	BR1	Ca—O	8	2.46(1)	0.006(1)
		Ca···O_{II}	13(2)	4.58(5)	0.04(1)
		Ca···Br	2	5.02(10)	0.05(2)
		Br···O	6	3.35(1)	0.012(1)
		O_w···O_w	2	2.89(1)	0.012(1)
$CaBr_2$(aq)	BR2	Ca—O	8	2.46(1)	0.006(1)
		Ca···O_{II}	11(2)	4.58(5)	0.04(1)
		Ca···Br	2	5.02(10)	0.05(2)
		Br···O	6	3.36(1)	0.011(1)
		O_w···O_w	2	2.87(2)	0.013(1)
$CaCl_2$(aq)	CL2	Ca—O	8	2.46(1)	0.006(1)
		Ca···O_{II}	11(2)	4.58(5)	0.04(1)
		Ca···Cl	2	4.90(10)	0.05(2)
		Cl···O	6	3.25(5)	0.009(1)
		O_w···O_w	2	2.89(1)	0.012(1)

[a] Parameters: distance d, number of distances n, mean-square displacement σ_l^2 of distance. The estimated standard deviations are given within parentheses for refined parameters. [b] Fixed parameter.

Table 4. Number of Molecules in the Different MD Simulations and Selected Parameters Obtained from the Ca^{2+}—O_w Radial Distribution Function

potential	n_{waters}	$n_{Ca^{2+}}$	n_{Cl^-}	concn (m)	$r_{Ca^{2+}-O_w}$, first max (Å)	$r_{Ca^{2+}-O_w}$, first min (Å)	$n_{Ca^{2+}-O_w}$ at first min
Åquist	509	1	2	0.11	2.39	3.33	7.9
Åquist	485	9	18	0.92	2.41	3.34	8.0
Bounds	509	1	2	0.11	2.51	3.42	9.5
GROMOS	509	1	2	0.11	2.46	3.31	8.0
GROMOS	485	9	18	0.92	2.46	3.36	8.1
GROMOS	458	18	36	1.76	2.46	3.36	8.1
GROMOS	431	27	54	2.51	2.46	3.38	8.0

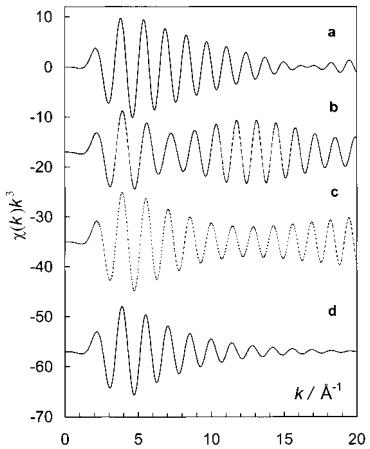

Figure 3. (a—c) Theoretically calculated EXAFS contributions for three individual snapshots (the top one with all Ca—O_w bond distances similar), and **(**d) averaged Ca K-edge theoretical spectrum (solid line) for 2000 configurations, from a simulation using the GROMOS potential.

3. Results and Discussion

3.1. Experimental Structure of the First Hydration Shell of Calcium and Halide Ions. 3.1.1. EXAFS Results. The k^3-weighted EXAFS spectrum of the 0.94 mol·dm^{-3} calcium(II) perchlorate solution is shown in Figure 1a, and for the 1.88 mol·dm^{-3} solution in Figure S1. The corresponding Fourier transform (FT) in Figure 1b is almost featureless for distances beyond the broad Ca—O_I peak. This shows that the single backscattering from the first hydration sphere is dominating in the part of the EXAFS region (k > 2.5 Å^{-1}) used for the FT, and that contributions from multiple scattering within the first sphere and the backscattering from the second sphere with longer pathways are of minor importance. By means of the FEFF7 program, the amplitude ratio was calculated for all possible multiple scattering pathways below 6 Å for a regular square antiprism of oxygen atoms around a calcium ion (Table S1). The result shows that the highest multiple scattering contribution should be from the four-leg Ca—O—Ca—O pathways of R = 4.92 Å (twice the Ca—O bond distance of 2.46 Å) with frequency 64 (Table S1), giving about 30% of the amplitude of the single Ca—O backscattering, for a Debye—Waller parameter $\sigma_e^2 = 0$ (i.e., stationary atoms) in a regular geometry. The calculation accounts for the effect of the mean-free-path factor, $\exp[-2R_j/\lambda(k)]$, and the inverse relation of the distance, $1/R_j^2$, on the EXAFS amplitude of the jth shell (with R_j instead of d in the EXAFS expression, eq 1). Together, these factors will reduce this four-leg Ca—O—Ca—O multiple scattering contribution relative to the single Ca—O backscattering, mostly at low k values (Figure S2b). In addition, the damping effect due to thermal and configurational disorder (the Debye—Waller factor) within the shell normally is higher for longer pathways, in particular at high k values (see Figure S2a).[23,48] Not only the multiple scattering but also the single Ca—O backscattering contribution from the second hydration shell, which has a very high σ_l^2 value in the Debye—Waller factor (cf. Table 3), is very strongly damped by disorder. Thus, the disorder in the first and second shells, which causes a considerable spread in the scattering pathways, is the reason for the lack of high r features in the Fourier transform.

Fourier filtering and back transformation of the Ca—O peak (solid curve in Figure 1a) reveal a distinct shoulder at k = 3.3 Å^{-1} in the experimental EXAFS spectra, which is present for all the aqueous solutions. This feature (probably due to multiple excitation) could not be described by calculated multiple scattering contributions and is not present in the MD simulated spectra which account for other low k features, cf. section 3.3. Therefore, model curve-fitting, both in k space and in r space, was done to the Fourier-filtered EXAFS function where this feature (and also possible multiple scattering contributions) has been eliminated, to extract the contributions from the first hydration shell only.

Curve-fitting of a single Ca—O shell in k space, assuming a symmetric (Gaussian) distribution of distances, revealed a phase shift at high k values, k > 7 Å^{-1} (Figures 1c and S1c), which indicates asymmetry.[23] This was accounted for in the model by including the third cumulant (eq 1), in an expansion of the distribution of Ca—O bond distances, which gave a satisfactory fit to the EXAFS function and increased the value for the centroid of the distances with about 0.03 Å (Table 2).

All structural parameters obtained for the Ca—O interaction are in close agreement for the three solutions studied (Table 2). The best fit was obtained for eight oxygen atoms in an asymmetric distribution around calcium at the Ca—O distance 2.46 ± 0.02 Å. The error given in the distance includes systematic deviations estimated from variations in the results from different samples and different conditions in the evaluation procedure, with the main effect originating from the uncertainty in the threshold energy E_0, about ±1.0 eV. The amplitude

(48) Lindqvist-Reis, P.; Eriksson, L.; Sandström, M.; Lidin, S.; Persson, I., unpublished results.

reduction factors, S_0^2, in Table 2 were obtained with apparently reasonable values for the solutions, 0.8−0.9. However, self-absorption and normalization problems for the fluorescence data,[25b] with increasing intensity due to decreasing absorption in the sample, lead to small S_0^2 values for the solids (Table 2), even though the experimental EXAFS oscillations were normalized by means of the spline and not the Victoreen function. For the solutions, the asymmetry of the Ca−O bond distribution can also affect the amplitude, and a good fit was obtained by fixing the Debye−Waller factor (σ^2) to the value obtained in the LAXS study and introducing a fourth cumulant accounting for the amplitude effect. This decreased the amplitude reduction factor, S_0^2, somewhat, without affecting the mean Ca−O distance (Table S2). Thus, the combined effects of the asymmetric distribution of distances, the unknown amplitude reduction factor, and the self-absorption make the uncertainty of the Debye−Waller factor rather large. However, the results are consistent with the value obtained from the LAXS data, for which only a symmetric distribution of the distances can be modeled.

3.1.2. LAXS Results. The LAXS radial distribution functions (RDFs) of the calcium halide solutions are dominated by the hydration of the anions. The hydrogen-bonded halide ion−water, X⁻···(H)−O(H), distances give rise to a major broad peak in the RDF at about 3.2, 3.4, and 3.6 Å for X = Cl, Br, and I, respectively (Figures 2 and S3). Increasing the size of the anion reduces the overlap with the minor contribution from the Ca−O_I distance at about 2.4 Å, and also with the hydrogen-bonded O···O distances in the bulk water at about 2.9 Å. A broad peak at about 4.6 Å is present in the RDFs of all solutions, consistent with second-sphere Ca···O_{II} distances.

For the first hydration sphere a consistent value of the Ca−O_I bond distance, 2.46(1) Å, was obtained by varying the structural parameters for the predominant contributions within reasonable limits, in the fitting of experimental and calculated structure-dependent intensity functions: $si(s)$, at high s values (eq 3). An eight-coordinated model, as found from the MD simulations (see below) with the water molecules in a distorted square antiprism around the calcium ion, gave a satisfactory fit. The parameter, σ_l, which corresponds to the rms deviation in the mean distance, is about 0.08(1) Å for Ca−O_I (Table 3). A model with nine coordination of the water oxygen atoms in a tricapped trigonal prism was also tested, but the two different Ca−O bond distances of this model converged to a single one at 2.46 Å, and the fit to the LAXS data did not improve.

Refinements of the X⁻···(H)−O(H) distances resulted in the mean values Cl⁻···O 3.25(1) Å, Br⁻···O 3.36(1) Å, and I⁻···O 3.61(1) Å (Table 3) for assumed coordination numbers of 6, 6, and 8, respectively. A change in the assumed coordination number affects the Debye−Waller parameter (Table 3) but not the distance significantly. The assumptions are based on previous results[2] and on the following considerations. The Cl⁻···O distance obtained for the chloride ion is somewhat longer than the mean value for a chloride ion octahedrally hydrogen-bonded to six water molecules, 3.15 Å in the crystal structure of $[ScCl_2(OH_2)_4]Cl{\cdot}2H_2O$ (see Figure S4a)[48] and 3.20 Å in $[YCl_2(OH_2)_6]Cl$.[49] A recent MD simulation of the iodide hydration resulted in a hydration number of 7.9 and a highest probability I⁻···O distance of 3.60 Å.[20] The average I⁻···O distance to the eight closest surrounding water molecules in the crystal structure of calcium iodide 6.5-hydrate was about 3.7 Å (cf. Figure S4b).[50]

Table 5. Comparisons between Experimentally Obtained Ca−O(aq) Bond Distances in Aqueous Solution and Three Sets of Correlated Coordination Numbers (N) and Ca−O Distances (d), Evaluated from Crystal Structures

coord no.	d_{Ca-O}−N correlation			sum of effective ionic radii[d]	experimental d_{Ca-O}(aq) (Å) in this study[e]
	first set[a]	second set[b]	third set[c]		
6	2.334(9)	2.35(1)	2.31−2.33	2.34	
7	2.403(5)	2.41(1)	2.40−2.41	2.40	
8	2.481(6)	2.45(1)	2.47−2.49	2.46	2.46 ± 0.01
9	2.521(4)	2.48(4)	2.53 (2.55−2.57)[f]	2.52	

[a] Reference 53. [b] Reference 11. [c] From hydrated Ca^{2+}(aq) ions in crystals (see text). [d] Shannon's radii for Ca (ref 67), with estimated radius of coordinated water molecule, 1.34 Å (ref 68). [e] Present EXAFS and LAXS results. [f] Nine-hydrates with six bridging waters.

This structure also displays octahydrated calcium ions with the mean Ca−O distance 2.47 Å (three oxygen atoms shared between the calcium ions) and 11 second-sphere Ca···I distances around each calcium ion in the range from 5.0 to 5.6 Å, mean value 5.30 Å.

3.1.3. Comparison with Hydrated Calcium Ions in Crystal Structures. In a wide distribution, the shorter Ca−O bond distances are expected to contribute more to the high k EXAFS data than the longer ones,[51] since shorter distances normally have smaller thermal disorder, and because of the inverse distance dependence of the EXAFS amplitude, $1/d_{Ca-O}^2$ (eq 1). The relative weights of the individual Ca−O contributions will then differ in various parts of the EXAFS spectra, in particular for a wide and asymmetric distribution. Therefore, the mean value obtained from an EXAFS or LAXS experiment may, to some extent, depend on the range of the scattering variable used in the evaluation of the results, and a direct comparison with an arithmetic average of the Ca−O bond distances should be used with some caution. However, for well-defined hydration shells the correlation between bond distances and coordination numbers is very useful in evaluations of EXAFS and LAXS data.[52]

Several compilations of Ca−O bond lengths in a large number of crystal structures have been made to correlate average distances to the coordination number n.[11,53] They include a wide range of oxygen-coordinated organic ligands in crystal structures in the Cambridge Structural Database. The spread was found to be large, and one survey based the evaluation of the expected mean values of the Ca−O bond distances on the sum of bond valences in the solid state.[53] A later analysis gave average Ca−O bond lengths as a function of the coordination number n (cf. Table 5).[11] Moreover, a number of reasonably well-determined crystal structures can be selected which contain discrete hydrated calcium(II) ions only surrounded by water molecules O_w, for hydration numbers from 6 to 9. All these structures display a more or less wide distribution of the Ca−O_w distances, but the arithmetic mean values were found to vary little for the same hydration number: Ca−6O_w 2.31−2.33 Å,[54−56] Ca−7O_w 2.40−

(49) Bell, A. M. T.; Smith, A. J. *Acta Crystallogr., Sect. C* **1990**, *46*, 960.
(50) Thiele, G.; Putzas, D. *Z. Anorg. Allg. Chem.* **1984**, *519*, 217.
(51) Zhang, H. H.; Hedman, B.; Hodgson, K. O. X-ray Absorption Spectroscopy and EXAFS Analysis: The Multiple Scattering Method and Application in Inorganic and Bioinorganic Chemistry. In *Inorganic Electronic Structure and Spectroscopy*; Solomon, E. I., Lever, A. B. P., Eds.; John Wiley and Sons: New York, 1999; Vol. I, Chapter 9.
(52) Lindquist-Reis, P.; Lamble, K.; Pattanaik, S.; Persson, I.; Sandström, M. *J. Phys. Chem. B* **2000**, *104*, 402.
(53) Carugo, O.; Djinović, K.; Rizzi, M. *J. Chem. Soc., Dalton Trans.* **1993**, 2127.
(54) Mazzarella, L.; Kovacs, A. L.; De Santis, P.; Liquori, A. M. *Acta Crystallogr.* **1967**, *22*, 65.
(55) Duhlev, R.; Brown, I. D. *Z. Kristallogr.* **1993**, *204*, 255.
(56) Simonsen, O. *Acta Chem. Scand.* **1997**, *51*, 861.

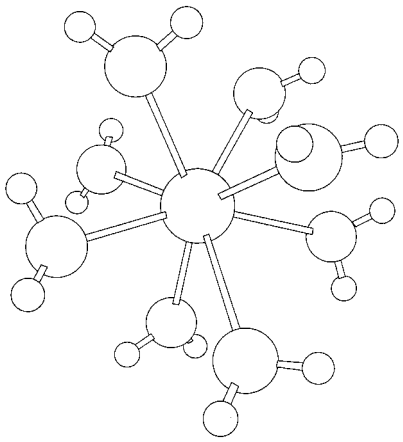

Figure 4. Typical snapshot of a distorted square antiprismatic $Ca(OH_2)_8$ configuration from an MD simulation with the GROMOS potential, with a large spread (2.36−2.68 Å) in the $Ca^{2+}-O_w$ bond distances.

2.41 Å,[57−60] Ca−8O_w 2.47−2.49 Å,[49,61−63] Ca−9O_w 2.53 Å (tricapped trigonal prism, 6 × 2.501, 3 × 2.579 Å),[64] and Ca−9O_w (with six bridging O_w) 2.55−2.57 Å.[65,66] Another correlation (Table 5) can be obtained from the effective ionic radii given by Shannon,[67] in combination with the estimated radius of the water molecule, 1.34 Å, derived from structure studies of the cesium alum salts.[68]

Thus, the mean Ca−O distance obtained from both the LAXS and EXAFS data, ca. 2.46 Å, clearly points to a hydration number of 8 in the solutions (Table 5). Six-coordination is definitively excluded, since also a high-level density functional theory calculation gave Ca−O 2.35 Å for a hexahydrated Ca^{2+} ion with a hydrogen-bonded second sphere of 12 water molecules.[12]

3.1.4. MD Simulation Results. All three $Ca^{2+}-OH_2$ interaction potentials used give a fairly well-defined first hydration shell, a second hydration shell, and some indication of a third hydration shell. The average Ca−O distances are about 2.40, 2.46, and 2.51 Å and the coordination numbers about 8, 8, and 9−10 for the Åqvist, GROMOS, and Bounds potentials, respectively (see Table 4). Both the Åqvist and the GROMOS potentials give rise to a characteristic coordination figure, a square antiprism, which is more or less maintained throughout the simulation. Figure 4 shows a snapshot for the GROMOS potential with a typical distance distribution and distorted coordination geometry. Bounds's potential gives a different coordination number and figure, namely nine-coordination in a tricapped trigonal prism (Figure S5a). Sometimes an extra water molecule takes part in the complex, giving 10-coordination in a bicapped square antiprism (Figure S5b).

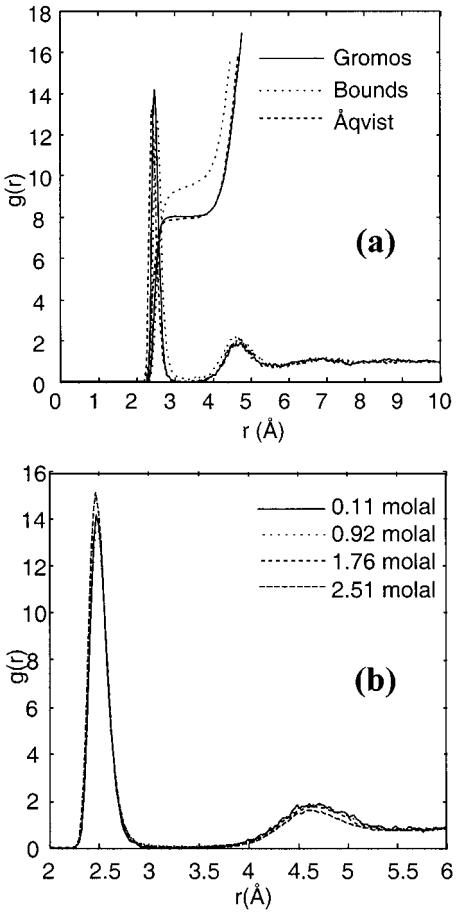

Figure 5. (a) Ca−O_w pair radial distribution functions for MD simulations of $CaCl_2$ solutions (0.11 *m*) with the GROMOS, Bounds, and Åqvist potentials. (b) Concentration dependence of the GROMOS simulations.

Figure 5a shows the $Ca^{2+}-O_w$ radial pair distribution function and the running coordination number for the three different potentials at 0.11 *m* concentration. The concentration dependence is shown for the GROMOS potential in Figure 5b. The variation for the different concentrations is small, and we therefore deduce that the water structure in the first hydration shell of the calcium ion is virtually concentration-independent, thereby justifying a comparison between the simulated and experimental EXAFS spectra, which were produced for slightly different concentrations.

We conclude that the GROMOS potential gives results which best agree with experiment, concerning both mean $Ca^{2+}-O$ distance and coordination number, thus justifying further comparison. In the following, most of our spectral analyses will be based on the GROMOS potential.

3.2. Thermal and Configurational Disorder of the Calcium Hydration. Spatial distribution functions were computed from the simulation with the GROMOS potential, to learn about both the average geometric coordination figure of water molecules and anions around the calcium ion and the relative cation−water motion. Figure 6a shows the location of oxygen atoms around the calcium ion in the 0.11 *m* solution, with the number of spheres proportional to the number density of oxygen atoms. Figure 6b shows the same spatial distribution function, represented as a "thermal" ellipsoid encompassing all the spheres. Table 6 gives the forms and sizes of these ellipsoids and the corresponding mean-square displacement values $<u_k^2>$. We have found that the smallest mean-square displacement component is approximately 0.020 $Å^2$; i.e., the rms displacement is

(57) Leligny, H.; Monier, J. C. *Acta Crystallogr., Sect. B* **1983**, *39*, 427.
(58) Takagi, S.; Mathew, M.; Brown, W. E. *Acta Crystallogr., Sect. C* **1984**, *40*, 1111.
(59) Thiele, G.; Rotter, H. W.; Faller, M. *Z. Anorg. Allg. Chem.* **1984**, *508*, 129.
(60) Faggani, R.; Villella, M.; Brown, I. D. *Acta Crystallogr., Sect. C* **1986**, *42*, 773.
(61) Dickens, B.; Brown, W. E. *Acta Crystallogr., Sect. B* **1972**, *28*, 3056.
(62) Leligny, H.; Monier, J. C. *Acta Crystallogr., Sect. B* **1982**, *38*, 355.
(63) Thiele, G.; Brodersen, K.; Pezzei, G. *Z. Anorg. Allg. Chem.* **1982**, *491*, 308.
(64) Burns, P. C.; Roberts, A. C.; Nikischer, A. J. *Eur. J. Mineral.* **1998**, *10*, 923.
(65) Agron, P. A.; Busing, W. R. *Acta Crystallogr., Sect. C* **1986**, *42*, 141.
(66) Leclaire, A.; Borel, M. M. *Acta Crystallogr., Sect. B* **1977**, *33*, 2938.
(67) Shannon, R. D. *Acta Crystallogr., Sect. A* **1976**, *32*, 751.
(68) Beattie, J. K.; Best, S. P.; Skelton, B. W.; White, A. H. *J. Chem. Soc., Dalton Trans.* **1981**, 2105.

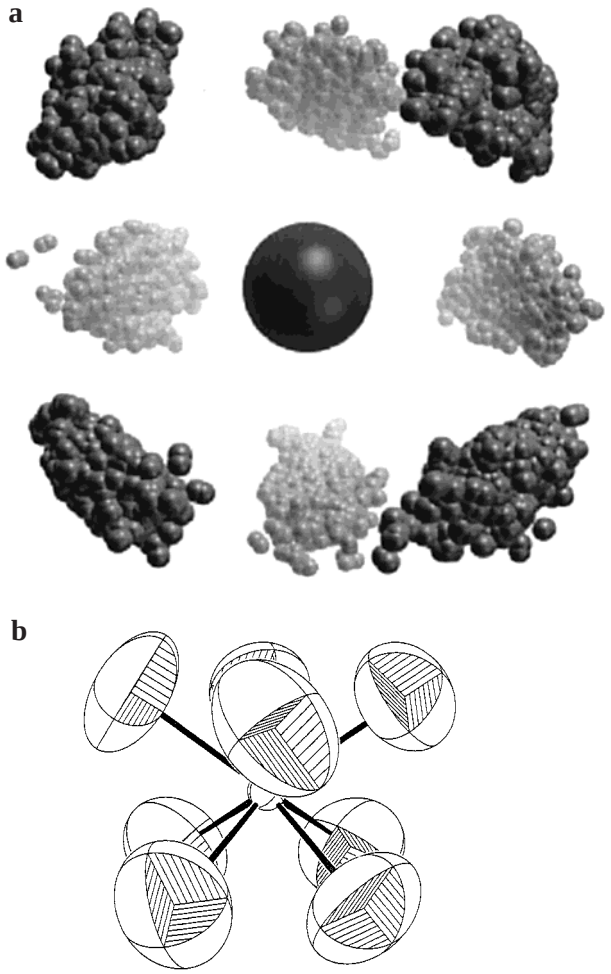

Figure 6. (a) Representation of coordination figures (2000 snapshots) for oxygen atom positions (small spheres) after rigid-body rotations (see text) for a simulation of 0.11 *m* $CaCl_2$ solution. (b) Ellipsoid representation (50% probability) of the oxygen atom positions.

Table 6. Thermal Parameters Extracted from the Spatial Distribution Functions for the Oxygen Atoms Coordinating the Calcium(II) Ion[a]

simulation	$\langle r_1 \rangle$ (Å)	$\langle u_1^2 \rangle$ (Å^2)	$\langle r_2 \rangle$ (Å)	$\langle u_2^2 \rangle$ (Å^2)	$\langle r_3 \rangle$ (Å)	$\langle u_3^2 \rangle$ (Å^2)
Åquist (0.11 *m*)	0.23	0.022	0.40	0.068	0.58	0.14
Åquist (0.92 *m*)	0.21	0.019	0.40	0.068	0.50	0.11
Bounds (0.25 *m*)	0.25	0.026	0.44	0.082	0.63	0.17
GROMOS (0.11 *m*)	0.20	0.017	0.42	0.075	0.52	0.11
GROMOS (0.92 *m*)	0.21	0.019	0.37	0.058	0.56	0.13
GROMOS (1.76 *m*)	0.22	0.020	0.44	0.082	0.57	0.14
GROMOS (2.51 *m*)	0.21	0.019	0.41	0.071	0.59	0.15
average		0.020		0.072		0.14

[a] If r_j is the length of the principal axis j (r_1 is the shortest) of one of the oxygen ellipsoids, then $\langle r_j \rangle$ is the average taken over all the first-shell ellipsoids. The corresponding mean-square displacement parameters $\langle u_j^2 \rangle$ are calculated as described in section 2.6. $\langle u_1^2 \rangle$ is thus similar to the σ_e^2 and σ_i^2 quantities from Tables 2 and 3, respectively.

0.14 Å. The corresponding rms values from the LAXS and EXAFS measurements are 0.08(1) and 0.10(2) Å, respectively. The MD results are thus slightly higher than the two experimental values, probably a result of encompassing an elongated, possibly banana-shaped, asymmetric cluster of spheres with an ellipsoid.

The smallest thermal displacement parameters obtained from the spatial distribution functions have also been compared with those that can be derived from the first peak in the Ca−O pair distribution function (Figure 5b), or rather from its unweighted probability equivalent. For the GROMOS potential, the half-width at half-height (HWHH) is 0.099 Å. If one assumes a Gaussian peak shape (although a blow-up of Figure 5b clearly shows asymmetry), its standard deviation can be calculated from the relation $\sigma(\ln 4)^{1/2} = 1.177\sigma = \text{HWHH}$, giving a thermal rms variation of ±0.084 Å for the Ca−O distance, close to the rms displacements obtained from the LAXS and EXAFS measurements. If we instead use a strategy as similar as possible to the calculation of $\langle u_k^2 \rangle^{1/2}$ from the thermal ellipsoids, where the maximum value of the distribution was used as the center and the largest deviation from the maximum determined the thickness of the ellipsoid, then the asymmetry of the $g(r)$ curve gives rise to an "equivalent" HWHH value of 0.132 Å. This gives a $\langle u^2 \rangle^{1/2}$ value of 0.11 Å along the Ca−O bond direction.

The thermal parameters from a large number of good-quality neutron diffraction studies of crystalline hydrates were analyzed in ref 69. For the water molecules, the oxygen out-of-plane vibrational amplitude was generally found to be higher than that for the in-plane vibrations, in particular for trigonally coordinated water molecules (as opposed to tetrahedrally coordinated ones). The smallest oxygen vibration at 300 K was found to be the in-plane vibration toward the ion ($\langle u_k^2 \rangle = 0.028$ Å^2 or $\langle u_k^2 \rangle^{1/2} = 0.17$ Å).[62] However, the crystal structure mean-square displacement amplitudes represent time and space averages of the oxygen atom *positions*.[46] Since this crystal structure amplitude is larger than the EXAFS, LAXS, and MD values obtained for the Ca−O bond distances in this work, this clearly shows an in-phase correlation between the atomic movements of the calcium ion and the water oxygen atoms in solution, giving rise to the smaller mean-square displacement amplitude.

3.3. Second Hydration Sphere of the Calcium Ion and Hydrogen Bonding. The LAXS radial distribution functions are clearly consistent with a second coordination sphere giving rise to distances between 4 and 5.5 Å for the calcium halide solutions studied (see Figure 2). Outside each hydrated Ca-$(H_2O)_8^{2+}$ complex, the stoichiometric water/halide molar ratio is in the range between 26.7/2.0 (BR1) and 15.4/2.2 (BR2) (cf. Table 1). In a random distribution of halide ions and water molecules, this means that at least one or two halide ions would be present in the second coordination sphere around each Ca-$(H_2O)_8^{2+}$ species. For the concentrated solutions, where sharing of second spheres occurs, the number becomes higher. The current MD simulations with the GROMOS potential give a second shell population of 16 waters for a cutoff at 5.3 Å, and 18.1 waters for a cutoff at 5.5 Å. We conclude that we have around 17 water molecules in the second hydration shell. Another recent MD simulation gave 17.6 second-shell waters with maximum probability at 4.46 Å from the calcium ion.[20]

Previously, a combined infrared spectroscopic and theoretical simulation study has been performed on the O−D stretching frequencies of isotopically isolated HDO molecules in aqueous electrolyte solutions.[70] The shift of the O−D stretching frequencies of water molecules affected by the ions was used to draw

(69) Eriksson A.; Hermansson K. *Acta Crystallogr., Sect. B* **1983**, *39*, 703.

(70) Lindgren, J.; Hermansson, K.; Wójcik, M. J. *J. Phys. Chem.* **1993**, *97*, 5254.

conclusions about the type and strength of the hydrogen bonding. Thus, the experimental IR results for a group of weakly hydrated ions, including calcium in 0.4 mol dm^{-3} perchlorate solution, could be explained assuming that there is a substantial amount of water molecules in the second shell *donating* hydrogen bonds to tetrahedrally (lone pair) coordinated first-shell water oxygen atoms.[70] This is consistent with results from neutron diffraction with isotopic substitution of calcium for concentrated $CaCl_2$ solutions (1.0, 2.8, and 4.5 *m*), showing the coordinated water molecules to be "tilted".[4] The mean "tilt" angles were found to be about 34−38° (tetrahedral coordination geometry corresponds to ∼55°). For these tilt angles, peaks at about 4.6 Å in the radial distribution function[4] can be interpreted as corresponding to $Ca\cdots O_{II}$ distances of linearly hydrogen-bonded ($O_I\cdots O_{II}$ at about 2.9 Å) second-shell water molecules.

The second coordination sphere was modeled in the LAXS data treatment by introducing $Ca\cdots O_{II}$ distances of 4.6 Å, and halide ions at the mean distances Ca···Cl 4.90 Å, Ca···Br 5.02 Å, and Ca···I 5.25 Å. These distances correspond to assumed tilt angles of the first-sphere water molecules of about 35°, with linear hydrogen bonds to the halide ions. The number of halide ions around this distance was varied up to four (twice the stoichiometric value) for the most concentrated solutions. Curve fitting in *r* space is then consistent with about 11 ± 2 and 13 ± 2 water molecules in the second sphere of the 2.0 and 1.5 mol dm^{-3} solutions, respectively, with a mean $Ca\cdots O_{II}$ distance of 4.58(5) Å (Table 3).

The mean hydrogen-bonded $O_w\cdots O_w$ distance between the water molecules was found to be close to 2.9 Å (Table 3), in agreement with previous studies.[22,24,52] A feature not explained by the models is a broad peak centered at about 4 Å, which appears in most RDF differences after subtraction of the model functions, and which increases with increasing CaX_2 concentration (cf. Figures 2 and S3). We have observed similar features for other concentrated aqueous electrolyte solutions and propose this feature to be due to a distribution of non-hydrogen-bonded O···O distances in a strongly perturbed water structure.

In our MD simulations of the calcium chloride solutions, the water molecules in the first shell are found to have preferentially trigonal orientation toward calcium, although with large flexibility of the configuration. The maximum probability of the second-sphere $Ca\cdots O_{II}$ distance is found at about 4.65 Å, slightly longer than the experimental result. This indicates a somewhat too strong directionality of the GROMOS potential, as also inferred from the Ca···Cl pair distribution function, which shows a high probability to find chloride ions about 5.2 Å from calcium (Figure S6). This distance is longer than the longest Ca···Cl distance, 5.1 Å, possible for a linear O_I—(H)···Cl hydrogen bond of 3.25 Å (the LAXS value) with trigonal coordination (no tilt) of the first-shell water molecules.

3.4. Theoretical EXAFS Spectra. EXAFS spectra for the MD simulations were computed as described in the Experimental and Computational Details, section 2.4.4. An experimental EXAFS spectrum is compared in Figure 7a with those theoretically calculated for the Bounds potential, and in Figure 7b to those for the GROMOS potential. We first note that the overall agreement between experiment and calculation is good in both cases. A closer inspection shows that the spectrum derived from the GROMOS potential follows the experimental one best, as expected from the agreement between the mean Ca−O distances.

The theoretical spectra in Figure 7 are generated from 2000 different instantaneous configurations (snapshots) of oxygen atoms around the calcium(II) ions and thus represent a space average for the hydrated calcium(II) ions. In the regular analysis of EXAFS data, the reduction of the amplitude of the EXAFS oscillations at high *k* values, caused by the thermally induced variation in bond distances, is taken into account by fitting a Debye−Waller factor in the model calculation for each type of distance. Our theoretical MD + FEFF analysis treats the thermal motion in a more direct way. The thermal motions (molecular diffusion, rotations, and rigid-body vibrations, but not intramolecular vibrations) of the water molecules and the ions are inherent in the MD simulation method, and the resulting snapshots (cf. Figure 3) thus sample the particle motion in a very realistic way (as realistically as the intermolecular potentials allow). Therefore, in the subsequent FEFF calculation of effective amplitudes for each backscattering pathway, no Debye−Waller factors were introduced. In this way also the multiple scattering contributions within the first shell are realistically accounted for, with their pathways distributed over a range of distances corresponding to the thermal and configurational disorder. The low *k* features in the experimental EXAFS spectra are reasonably well described (cf. Figure 7), except for the distinct shoulder at about 3.3 $Å^{-1}$, which may be caused by a multiple excitation of a similar type as found previously in EXAFS spectra of, e.g., strontium, barium, yttrium, and lanthanum.[22,52,71]

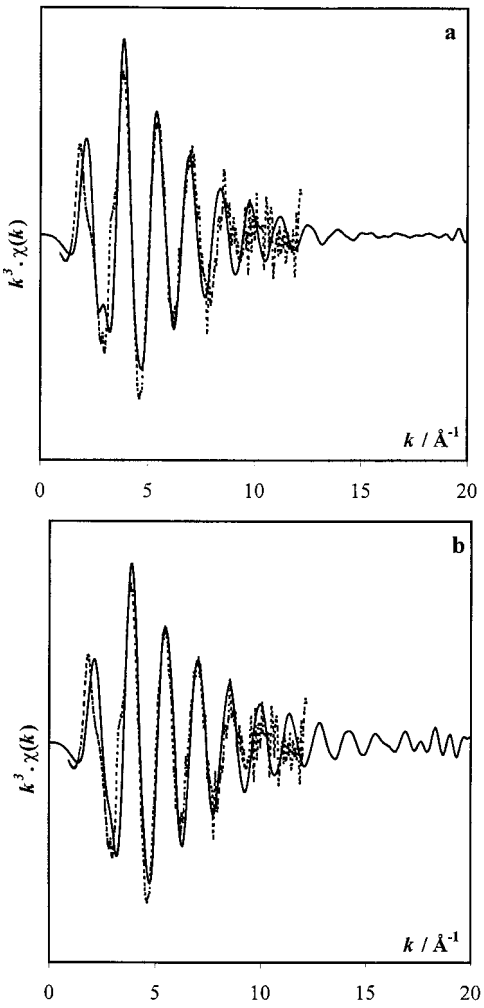

Figure 7. Comparison of the Ca K-edge EXAFS spectrum for the 0.94 mol dm^{-3} $Ca(ClO_4)_2$ aqueous solution (dashes) with (a) simulated spectrum with Bounds's potential and (b) GROMOS potential.

(71) Näslund, J.; Lindqvist-Reis, P.; Persson, I.; Sandström, M. *Inorg. Chem.* **2000**, *39*, 4006.

Although the experimental spectra correspond to the average theoretical spectrum as displayed in Figure 7, we find it useful to be aware of the very large variations in the individual contributing interference patterns (as shown in Figure 3), which together make up the total theoretical (and experimental) spectra. Since we find that the magnitudes of our computed $\langle u_k^2 \rangle$ values agree well with experiment, without using any thermal or disorder parameters apart from the ones implicit in the MD method, we have reason to believe that the large variations shown in Figure 3 are realistic.

4. Conclusions

The combined results, and the correlation between the experimental mean Ca−O distances in solution, in crystal structures, and from MD simulations, are all consistent with an eight coordination of the hydrated calcium(II) ion in aqueous solution with the Ca−O bond distances centered around 2.46 Å in a wide distribution, with an rms variation of about ±0.09 Å. The EXAFS data, which give higher spatial resolution than LAXS, show the distribution of the Ca−O bond distances to be somewhat asymmetric. The introduction of a third cumulant in the EXAFS model, to account for the asymmetry in the probability distribution of the individual Ca−O bond distances, increased the mean Ca−O distance by about 0.03 Å as compared to a symmetric (Gaussian) distribution model. Thus, the mean value, or the centroid of the distribution,[30] becomes to some extent dependent on the technique and model used, because of the different weighting of the individual contributions. No concentration dependence of the coordination geometry or number could be found for the relatively concentrated solutions studied (experimentally 0.94−2.0 mol·dm^{-3}, MD simulations 0.11−2.51 *m*).

The LAXS results show a second hydration sphere with mean Ca···O_{II} distances of about 4.58(5) Å and rms variations of ±0.20(3) Å, and with solvent-shared ion pairs of halide ions, in approximately expected stoichiometric ratios. Also, the MD results show hydrogen-bonded second hydration spheres. In the simulation using the potential from the GROMOS program for a 2.51 *m* $CaCl_2$ solution, i.e., with the molar ratio H_2O/Cl = 8.0/2.0 outside each octahydrated calcium ion (Table 4), each calcium(II) ion is, on the average, surrounded by about four chloride ions at a distance in the range 4.5−6 Å (Figure S6c). This implies a substantial sharing of halide ions between the second hydration shells of neighboring calcium ions.

One important result of this work is that we have found it possible to calculate realistic theoretical EXAFS spectra for aqueous calcium chloride solutions by linking the FEFF program to an MD simulation. Moreover, MD results provide structural and dynamic molecular-level detail beyond what is possible to obtain experimentally. Provided the underlying intermolecular potentials are reliable, such detailed results give extremely valuable information concerning ion−water hydration, in particular in a case like the current with relatively weak hydration leading to configurational disorder in the first shell.

Acknowledgment. We gratefully acknowledge the Swedish Natural Science Research Council and the Foundation for Strategic Research (SSF) for financial support and the Stanford Synchrotron Radiation Laboratory (SSRL) for allocation of beam time and laboratory facilities. SSRL is operated by the Department of Energy, Office of Basic Energy Sciences. The SSRL Biotechnology Program is supported by the National Institutes of Health, National Center for Research Resources, Biomedical Technology Program, and by the Department of Energy, Office of Biological and Environmental Research.

Supporting Information Available: Table S1, calculated amplitude ratio of multiple scattering pathways for a regular square antiprismic CaO_8 coordination; Table S2, results of EXAFS *k* space model fitting of the first coordination shell of the calcium(II) ion in a 0.94 mol dm^{-3} solution of $Ca(ClO_4)_2$; Figure S1, experimental Ca K-edge EXAFS data for 1.88 mol dm^{-3} $Ca(ClO_4)_2$ aqueous solution, Fourier transform, Fourier-filtered back-transform, and model fitting in *k* space; Figure S2, Debye−Waller factors for different σ^2 and amplitude reduction caused by the mean-free-path factor and the $1/R^2$ dependence; Figure S3, LAXS radial distribution functions for a 1.5 mol·dm^{-3} $CaBr_2$ solution (BR1); Figure S4, a chloride ion octahedrally hydrogen bonded to six water molecules and hydrated iodide ions (average I^-···O distance 3.7 Å) and octahydrated calcium ions (mean Ca−O distance 2.37 Å) in the crystal structure of CaI_2·6.5H_2O; Figure S5, MD snapshots from a simulation with Bounds's potential, with tricapped trigonal prismatic configuration of $Ca(OH_2)_9$ species and the bicapped square antiprism occasionally formed of $Ca(OH_2)_{10}$ species; Figure S6, Ca−Cl pair distribution functions from MD simulations of $CaCl_2$ aqueous solution (PDF). This material is available free of charge via the Internet at http://pubs.acs.org.

JA001533A